



Extracellular Vesicles Improve Post-Stroke Neuroregeneration and Prevent Postischemic Immunosuppression

THORSTEN R. DOEPPNER,^{a,b,*} JOSEPHINE HERZ,^{a,c,*} ANDRÉ GÖRGENS,^b JANA SCHLECHTER,^a ANNA-KRISTIN LUDWIG,^b STEFAN RADTKE,^b KYRA DE MIROSCHEJJI,^b PETER A. HORN,^b BERND GIEBEL,^b DIRK M. HERMANN^a

Key Words. Adult stem cells • Angiogenesis • Cellular therapy • Clinical translation • Mesenchymal stem cells • Nervous system • Tissue regeneration

^aDepartment of Neurology, ^bInstitute for Transfusion Medicine, and ^cDepartment of Pediatrics I, University Hospital Essen, University of Duisburg-Essen, Essen, Germany

* Contributed equally.

Correspondence: Thorsten R. Doeppner, M.D., Department of Neurology, University Hospital Essen, Hufelandstrasse 55, Essen 45147, Germany. Telephone: 201-723-83586; E-Mail: thorsten.doeppner@uk-essen.de; or Bernd Giebel, Ph.D., Institute for Transfusion Medicine, University Hospital Essen, Virchowstrasse 179, Essen 45147, Germany. Telephone: 201-723-4204; E-Mail: bernd.giebel@uk-essen.de

Received April 20, 2015; accepted for publication June 24, 2015; published Online First on September 3, 2015.

©AlphaMed Press
1066-5099/2015/\$20.00/0

<http://dx.doi.org/10.5966/sctm.2015-0078>

ABSTRACT

Although the initial concepts of stem cell therapy aimed at replacing lost tissue, more recent evidence has suggested that stem and progenitor cells alike promote postischemic neurological recovery by secreted factors that restore the injured brain's capacity to reshape. Specifically, extracellular vesicles (EVs) derived from stem cells such as exosomes have recently been suggested to mediate restorative stem cell effects. In order to define whether EVs indeed improve postischemic neurological impairment and brain remodeling, we systematically compared the effects of mesenchymal stem cell (MSC)-derived EVs (MSC-EVs) with MSCs that were i.v. delivered to mice on days 1, 3, and 5 (MSC-EVs) or on day 1 (MSCs) after focal cerebral ischemia in C57BL6 mice. For as long as 28 days after stroke, motor coordination deficits, histological brain injury, immune responses in the peripheral blood and brain, and cerebral angiogenesis and neurogenesis were analyzed. Improved neurological impairment and long-term neuroprotection associated with enhanced angioneurogenesis were noticed in stroke mice receiving EVs from two different bone marrow-derived MSC lineages. MSC-EV administration closely resembled responses to MSCs and persisted throughout the observation period. Although cerebral immune cell infiltration was not affected by MSC-EVs, postischemic immunosuppression (i.e., B-cell, natural killer cell, and T-cell lymphopenia) was attenuated in the peripheral blood at 6 days after ischemia, providing an appropriate external milieu for successful brain remodeling. Because MSC-EVs have recently been shown to be apparently safe in humans, the present study provides clinically relevant evidence warranting rapid proof-of-concept studies in stroke patients. *STEM CELLS TRANSLATIONAL MEDICINE* 2015;4:1131–1143

SIGNIFICANCE

Transplantation of mesenchymal stem cells (MSCs) offers an interesting adjuvant approach next to thrombolysis for treatment of ischemic stroke. However, MSCs are not integrated into residing neural networks but act indirectly, inducing neuroprotection and promoting neuroregeneration. Although the mechanisms by which MSCs act are still elusive, recent evidence has suggested that extracellular vesicles (EVs) might be responsible for MSC-induced effects under physiological and pathological conditions. The present study has demonstrated that EVs are not inferior to MSCs in a rodent stroke model. EVs induce long-term neuroprotection, promote neuroregeneration and neurological recovery, and modulate peripheral post-stroke immune responses. Also, because EVs are well-tolerated in humans, as previously reported, the administration of EVs under clinical settings might set the path for a novel and innovative therapeutic stroke concept without the putative side effects attached to stem cell transplantation.

INTRODUCTION

The delivery of somatic stem cells induces unique restorative responses in the adult brain, reducing brain injury and promoting functional neurological recovery in animal models of cerebral ischemia [1–12]. The beneficial effects are not restricted to single stem cell lineages but have been reported for a huge

variety of adult stem cells and progenitor cells alike. In terms of clinical feasibility, the transplantation of mesenchymal stem cells (MSCs) is particularly attractive because they can be easily obtained and thus offer the opportunity for autologous and allogeneic stem cell transplantation [13]. Consequently, the first clinical trials using MSC transplantation for ischemic stroke treatment have been initiated [14–18].

Although the initial concepts aimed to replace lost brain tissue, recent evidence has suggested that stem cells exert their restorative effects via indirect bystander actions. These include a variety of different processes such as the prevention of secondary neuronal degeneration, modulation of peripheral and central immune responses, and promotion of cerebral angiogenesis [1, 12, 19–21]. In line with this, most systemically grafted MSCs are trapped within the lungs, again suggesting a paracrine method of action for the transplanted cells [22, 23]. Conditioned MSC media exert similar beneficial effects in a model of myocardial infarction-like MSCs [24]. Consistently, MSCs have been reported to secrete survival-promoting factors that enhance angiogenesis [25–27]. On processing of conditioned MSC media, small extracellular vesicles (EVs) such as exosomes (70–160 nm in diameter) were identified. The latter have subsequently been proved to exert beneficial therapeutic effects in models of myocardial ischemia, liver fibrosis, kidney injury, and cerebral ischemia [28–32].

Exosomes are defined as derivatives of the late endosomal compartment. They correspond to the intraluminal vesicles of multivesicular bodies, which, on fusion with the plasma membrane, release these vesicles as exosomes into the environment. Together with other small EVs such as microvesicles (100–1,000 nm), which bud off from the plasma membrane, exosomes can be highly enriched by processing cell culture supernatants or body liquids [33, 34]. Exosome-enriched EV fractions in turn contain coding and noncoding RNAs, lipids, and proteins [35] and play pivotal roles in intercellular communication processes [36].

Although no experimental evidence has been obtained that administration of MSCs causes any critical side effects in treating cerebral ischemia in rats [37], it cannot be excluded that MSCs might cause occlusions of small vessels [38]. Also, although evidence regarding the malignant transformation of grafted MSCs does not yet exist, a theoretic malignant transformation, such as is already known from embryonic and related stem cells, cannot be excluded [39–41]. Because malignant transformation after EV administration is extremely unlikely, EV therapies could provide a number of advantages over conventional stem cell therapies, provided they are as effective as cellular therapies.

After showing that MSC-EVs exert immunosuppressive functions *in vitro*, we recently treated a patient with steroid-refractory graft-versus-host-disease (GvHD) with MSC-EVs [42]. As previously reported for MSC therapy in GvHD patients [43], MSC-EV treatment suppressed GvHD symptoms without inducing any side effects [42]. To evaluate the therapeutic potential of MSC-EVs for treatment of ischemic stroke, we systematically compared the effects after MSC-EV and MSC administration on neurological recovery and brain remodeling in a mouse model of transient focal cerebral ischemia. Our data show that MSC-EV administration closely mimics the beneficial effects after MSC treatment in stroke. Furthermore, by studying the mechanistic effects of MSC-EVs, we obtained evidence that MSC-EVs attenuate peripheral immunosuppression and promote both neuronal survival and angiogenesis. Our data thus support the use of MSC-EVs for stroke treatment.

MATERIALS AND METHODS

Experimental Setting and Animal Groups

All studies were performed with governmental approval according to NIH guidelines for the care and use of laboratory animals. Male C57BL6 mice aged 10 weeks (Harlan Laboratories, Darmstadt,

Germany, <http://www.harlan.com>) were kept under circadian rhythm with free access to food and water. The mice were randomly assigned to the treatment groups. At all stages of the study, the researchers were kept unaware of the experimental conditions chosen.

Middle cerebral artery occlusion (MCAO) was induced, as described previously [22]. In brief, a silicon-coated monofilament (Doccol Corp., Sharon, MA, <http://www.doccol.com>) was inserted into the left common carotid artery (CCA) and then gently pushed forward toward the offspring of the left middle cerebral artery (MCA). During the experiment, the laser Doppler flow (LDF) was recorded with a flexible probe (Perimed AB, Järfälla, Sweden, <http://www.perimed-instruments.com>) above the core of the left MCA territory. Thirty minutes after monofilament insertion, reperfusion was initiated by monofilament removal, and the LDF recordings were continued for an additional 15 minutes before the wounds were carefully sutured.

The first set of mice was exposed to MCAO followed by administration of normal saline (control), MSCs (1×10^6 cells per 250 μ l of saline), or MSC-EVs (EVs released by 2×10^6 MSCs diluted in 250 μ l of saline). The cells were transplanted 24 hours after stroke via cannulation of the right femoral vein in the anesthetized mice. The injections of the saline-treated and MSC-EV-treated groups were repeated 3 and 5 days after ischemia (DPI). The mice in the MSC group received saline injections at 3 and 5 DPI. All samples were injected at a rate of 250 μ l/10 min. The mice were allowed to survive for 28 DPI (12 mice per group). These mice were used for the behavioral analyses and histochemical studies of brain injury and angiogenesis.

The second set of mice underwent sham surgery or MCAO followed by delivery of saline (control) or MSC-EVs of 1 of the MSC lines at 24 hours after ischemia. In the sham-operated mice, all the procedures were performed exactly as for MCAO except for occlusion of the MCA. As such, the left CCA and external carotid artery were isolated and ligated, and a small incision was made in the left CCA, followed by immediate ligation without introducing a filament. The sham-operated mice received saline injections. All these groups were allowed to survive for 48 hours after ischemia (8 mice per group). The peripheral blood cells of these mice were harvested and analyzed by flow cytometry. The brains were used for histochemical analysis of infarct volumes and for determination of brain inflammation.

The third set of mice underwent sham surgery or MCAO, followed by delivery of saline (control) or MSC-EVs at 24 hours after ischemia and 3 and 5 DPI. These mice were allowed to survive for 6 DPI (12 mice per group). These mice were used for flow cytometry analysis of leukocyte subsets within the blood and within the brain at 6 DPI.

The fourth set of mice was subjected to focal cerebral ischemia, followed by delivery of saline (control) or MSC-EVs at 24 hours after ischemia and 3 and 5 DPI. These mice were allowed to survive for 6 DPI (8 mice per group). The brains of these mice were prepared and used for histochemical analysis to determine the infarct volumes and brain inflammation at 6 DPI.

Thus, a total of 116 animals were included in the present study protocol. Of these mice, 8 mice (3 saline treated, 2 MSC treated, and 3 EV treated) had to be excluded from the study because of predefined exclusion criteria, including surgery duration longer than 15 minutes, a lack of reperfusion after filament withdrawal, or spontaneous animal death.

Expansion and Characterization of MSCs

Bone marrow (BM) was obtained from human donors after informed consent according to the Declaration of Helsinki. Cells were fractionated by Ficoll (Bicoll Separating Solution; Biochrom AG, Berlin, Germany, <http://www.biochrom.de>) density gradient centrifugation and seeded into tissue culture 6-well plates (2×10^6 cells per well) in MSC basal media (Pan-Biotech, Aidenbach, Germany, <http://www.pan-biotech.de>) supplemented with 5% human thrombocyte lysate, 1% glutamine, and 1% penicillin-streptomycin (Invitrogen, Darmstadt, Germany, <http://www.lifetechnologies.com>). After 24 hours, nonadherent cells were removed by medium exchange. After cell confluence, the cells were continuously passaged. MSCs were characterized by flow cytometric analysis.

The MSCs were stained with fluorescein isothiocyanate-conjugated, phycoerythrin-conjugated or allophycocyanin-conjugated anti-CD90 (clone 2G5; Beckman Coulter, Fullerton, CA, <http://www.beckmancoulter.com>), anti-CD105 (clone sN6/N1-3A1; Ancell, Bayport, MN, <http://www.ancell.com>), anti-CD14 (clone M5E2; BD Biosciences, Heidelberg, Germany, <http://www.bd.com>), anti-CD31 (clone WM59; BD Biosciences), anti-CD73 (clone AD2; BD Biosciences), anti-CD146 (clone TEA1134; Beckman Coulter), anti-CD44 (clone G44-26; BD Biosciences), or anti-CD45 (clone J33; Beckman Coulter) antibodies for 20 minutes at 4°C. Propidium iodide was used for exclusion of dead cells. Appropriate isotype-matched control monoclonal antibodies were used to determine the level of background staining in all experiments. Flow cytometric analyses were performed on a FC500 flow cytometer equipped with CXP, version 2.2, software (Beckman Coulter).

To test for osteogenic differentiation patterns (supplemental online Fig. 1), 4×10^4 MSCs were plated onto 12-well plates and raised until they reached 80%–90% confluence. Osteogenic differentiation was induced by the addition of Dulbecco's modified Eagle's medium (DMEM) high glucose medium (PAA Laboratories, Cölbe, Germany, <http://www.atmp-ready.com>) supplemented with 10% fetal bovine serum (FBS; Biochrom GmbH, Berlin, Germany, <http://www.biochrom.de>), 1% sodium pyruvate (Sigma-Aldrich, Germany, <http://www.sigmaaldrich.com>), 1% glutamine, 1% penicillin-streptomycin (Invitrogen), 0.1 μ M dexamethasone, 10 mM β -glycerol-phosphate, and 300 mM ascorbic acid (Sigma-Aldrich). The medium was exchanged twice a week. After 2 weeks, the cells were fixed at room temperature (RT) for 20 minutes in 4% paraformaldehyde (Sigma-Aldrich) and stained with alizarin red (2% wt/vol in water, pH 4.2; Carl Roth, Karlsruhe, Germany, <http://www.carlroth.com>).

Adipocyte differentiation (supplemental online Fig. 1) was induced by the addition of DMEM high-glucose medium (PAA Laboratories) supplemented with 10% FBS (Biochrom), 1% sodium-pyruvate (Sigma-Aldrich), 1% glutamine, 1% penicillin-streptomycin (Invitrogen), 0.1 μ M dexamethasone, and 200 μ M indomethacin (Sigma-Aldrich). The medium was exchanged twice a week. After the first medium exchange, the adipocyte differentiation medium was additionally supplemented with 2 μ M insulin and 500 μ M 3-isobutyl-1-methylxanthine (Sigma-Aldrich). After fixation (4% paraformaldehyde for 20 minutes at RT), the cells were stained with 0.4% Oil Red O (Sigma-Aldrich) diluted in isopropanol.

Enrichment and Infusion of EVs From Conditioned MSC Media

After passage 3, MSC-conditioned media (CM) were collected every 48 hours. Larger vesicles and debris were removed by

filtration through 0.22- μ m pore filters (TPP Techno Plastic Products AG, Trasadingen, Switzerland, <http://www.tpp.ch>). CM were stored at -20°C until processing. After thawing, CM were unified and supplemented with 3 U/ml heparin (Ratiopharm GmbH, Ulm, Germany, <http://www.ratiopharm.de>) and 3 μ g/ml Actilyse (Boehringer Ingelheim GmbH, Ingelheim, Germany, <http://www.boehringer-ingelheim.com>) and incubated for 3 hours at 37°C . EVs were concentrated by a polyethyleneglycol (PEG) precipitation method as previously described [42]. In brief, PEG precipitation was performed at a final concentration of 10% PEG6000 (50% wt/vol; Sigma-Aldrich) and 75 mM NaCl. After incubation for 8–12 hours at 4°C , the EVs were concentrated by centrifugation for 30 minutes at 1,500g. EV pellets were resolved in normal saline (B. Braun Melsungen, Melsungen, Germany, <http://www.bbraun.com>), filled with saline (if not explicitly stated, using normal saline) to a total volume of 45 ml and precipitated by ultracentrifugation for 2 hours at 110,000g. EV pellets were resolved and diluted in saline to a concentration of 1 ml containing EVs obtained from CM of 4×10^7 MSCs. Aliquots of 1 ml each were stored at -80°C until usage.

EV samples were tested for bacterial contamination via polymerase chain reaction and infectious serology, as described previously [42]. All EV samples used were negative in all assays. For the characterization of EV samples, nanoparticle tracking analyses were performed with the ZetaView platform (Particle Metrix, Meerbusch, Germany, <http://www.particle-metrix.com>). As shown previously, 1:500 or 1:1,000 water-diluted samples were measured in duplicate [44].

Protein concentrations of EV samples were determined using the micro-bicinchoninic acid assay (Thermo Fisher Scientific, Dreieich, Germany, <http://www.thermofisher.com>). Western blots were performed with 5 μ g of the concentrated EV fractions, which were treated with sample buffer (dithiothreitol, 0.1% SDS, 0.1 M Tris HCl; pH 7.0) and boiled for 5 minutes at 95°C before separation on 12% SDS-polyacrylamide gel electrophoresis gels. The samples were transferred to polyvinylidene fluoride membranes (Merck Millipore, Darmstadt, Germany, <http://www.merckmillipore.com>). Membranes were stained with antibodies recognizing either the exosomal marker proteins Tsg101 (Sigma-Aldrich) or CD81 (BD Biosciences).

Analysis of Post-Stroke Motor Coordination Deficits

The mice were trained on days 1 and 2 before induction of stroke to ensure proper test behavior. The actual tests for analysis of motor coordination were performed at the time points given using the rotarod, tightrope, and corner turn test, as previously described [45]. Both the rotarod and tightrope tests were performed twice on each test day and the mean values calculated. For the rotarod test, the readout parameter was the time until the mice dropped off, with a maximal testing time of 300 seconds. Assessment of tightrope test results was done using a validated score ranging from 0 (minimum) to 20 (maximum). The corner turn test included 10 trials per test day, during which the laterality index (number of right turns per 10 trials) was calculated. High laterality indexes approximating a score of 1 indicate severe motor coordination impairment.

Immunohistochemical Tissue Processing and Staining

For the measurement of infarct volumes and immunohistochemical analysis, the mice were transcardially perfused with

phosphate-buffered saline (PBS) after having been anesthetized with 7% chloral hydrate (200 mg/kg body weight). The brains were removed, shock frozen, and cut into 20- μ m-thick coronal sections. To determine the infarct volumes, every 20th section (i.e., sections at 400- μ m distance) was stained with cresyl violet, followed by a computer-based analysis of the infarct volumes. Infarct volumes were determined, as described previously [46], by subtracting the nonlesioned volume of the ipsilateral hemisphere from the total volume of the contralateral side.

Long-term neuronal survival was evaluated in 20- μ m sections stained with a mouse monoclonal anti-NeuN antibody (1:1,000; Merck Millipore), which was detected by a goat anti-mouse Alexa Fluor 488 antibody (Invitrogen). For analysis, the regions of interests (ROIs) were defined at anteroposterior +0.14 mm, medial-lateral \pm 1.5 to 2.25 mm, and dorsal-ventral $-$ 2.5 to 3.25 mm. Two sections per mouse were analyzed, and in each section, three ROIs were examined. The mean neuronal densities were determined for all ROIs. Leukocyte infiltrates were analyzed in 20- μ m sections stained with a rat anti-mouse CD45 antibody (clone IBL-5/25, 1:100; Merck Millipore), which was detected with a donkey anti-rat Alexa Fluor 488 antibody (Invitrogen). The density of CD45⁺ leukocytes was evaluated in the same ROI as above, again using two sections per mouse. The mean densities of leukocytes were determined for all ROIs.

Endogenous cell proliferation and differentiation of newborn cells were analyzed after daily single i.p. injection of 5-bromo-2-deoxyuridine (BrdU; 50 mg/kg body weight; Sigma-Aldrich) on days 8–18. The sections were counterstained for BrdU and doublecortin (Dcx; immature neuronal marker), NeuN (mature neuronal marker), or CD31 (endothelial marker). A monoclonal mouse anti-BrdU (1:400; Roche Diagnostics, Basel, Switzerland, <http://www.roche-applied-science.com>), a monoclonal rat anti-BrdU (1:400; Abcam, Cambridge, U.K., <http://www.abcam.com>), a polyclonal goat anti-Dcx (1:50; Santa Cruz Biotechnology, Heidelberg, Germany, <http://www.scbt.com>), a monoclonal mouse anti-NeuN (1:1,000; Merck Millipore), and a monoclonal rat CD31 (1:200, BD Biosciences) antibody were used. All primary antibodies were detected using appropriate Cy-3-labeled, Alexa Fluor 594-labeled, or Alexa Fluor 488-labeled secondary antibodies.

Processing of Peripheral Blood and Brain Tissue for Flow Cytometry

Single cell suspensions for flow cytometry were performed, as described previously [47]. In brief, the mice were killed via i.p. injection of chloral hydrate. Blood samples were collected into EDTA-coated tubes by puncture of the inferior vena cava followed by transcardial perfusion with ice-cold 0.1 M PBS and brain removal. Absolute white blood cell (WBC) counts of whole blood samples were determined using a veterinary hematology analyzer (scil Vet abc Plus; scil animal care co., Vierhnhelm, Germany, <http://www.scilvet.com>). Erythrocytes were lysed by incubation with lysis buffer (155 mM NH₄Cl, 10 mM KHCO₃, 3 mM EDTA) for 5 minutes followed by 2 washing steps with 0.1 M PBS. The brains were dissected and hemispheres divided into ipsilesional and contralesional parts. For each measurement, 4 hemispheres were pooled and homogenized through a 70- μ m cell strainer (BD Biosciences) by continuous rinsing with 50 ml of cold HEPES-buffered Roswell Park Memorial Institute 1640. The samples were centrifuged at 286g for 5 minutes at 18°C. The supernatants were

discarded and the pellets resuspended in 15 ml of 37% Percoll in 0.01 M HCl/PBS and centrifuged at 2,800g for 20 minutes. Myelin was removed, and the remaining cell pellet was washed twice in 0.01 M PBS.

Flow Cytometry

Isolated cells were incubated with the blocking antibody rat anti-mouse CD16/CD32 (Fc fragment) for 15 minutes at 4°C, followed by incubation with the antibodies listed in supplemental online Table 1 for an additional 30 minutes. Absolute cell numbers in the blood were calculated by the multiplication of the WBC count per microliter and the percentage of individual subpopulations. Total counts of brain-infiltrating leukocytes were determined using TrueCount beads (BD Biosciences) on the basis of CD45-positive events.

Blood- and brain-derived leukocyte subsets were identified and differentiated by their antigen expression using multichannel flow cytometry (supplemental online Fig. 2). Single cells were identified by forward and side scatter (area vs. width) parameters, followed by gating for CD45-positive cells in the blood (supplemental online Fig. 2A, 2B) and for CD45^{high} cells in the brain (supplemental online Fig. 2C). These cells were further divided into lymphoid cells (B cells [B220], natural killer [NK] cells, and CD4 and CD8 T cells; supplemental online Fig. 2B) and myeloid cells, including neutrophils (lineage-negative, Ly6G⁺), macrophages (lineage-negative, Ly6G⁻, SSC^{low}, CD115⁻, CD11b⁺), monocytes (lineage-negative, Ly6G⁻, SSC^{low}, CD115⁺), and dendritic cells (lineage-negative, Ly6G⁻, SSC^{low}, CD115⁻, CD11c^{high}; supplemental online Fig. 2A). Two panels of antibodies were used (supplemental online Table 1). Panel 1 enabled analysis of myeloid-derived leukocytes, which further allowed the determination of activation levels of monocytes and dendritic cells via major histocompatibility class II (MHCII) expression and the differentiation between monocyte subsets according to their Ly6C expression level (supplemental online Fig. 2A). Panel 2 divided lymphocytes and further enabled examination of lymphocyte subset activation via CD69 expression (supplemental online Fig. 2B). For each panel, a negative control (panel 1, stained for all antigens except for MHCII; panel 2, stained for all antigens except for CD69) was included to define the positive populations.

Statistical Analysis

For comparison of two groups, two-tailed independent Student's *t* tests were used. For comparison of three or more groups, one-way analysis of variance (ANOVA) followed by Tukey's post hoc test and, if appropriate, two-way ANOVA were used. Unless otherwise stated, data are presented as mean \pm SD values. *P* \leq .05 was considered statistically significant.

RESULTS

Delivery of MSC-EVs Reduces Postischemic Motor Coordination Impairment as Effectively as MSC Delivery

Because MSC-EVs are proposed to be critically involved in MSC-induced therapeutic effects after stroke, we systematically compared the recovery-promoting effects of two independent MSC lines and their corresponding MSC-EV fractions on neurological recovery after stroke. MSCs were raised from BM samples of two different human BM donors (supplemental online Fig. 1), and their MSC-EV fractions were characterized according to current standards. MSCs or their corresponding EVs were i.v. infused

in mice at 1 DPI (MSCs) or at 1, 3, and 5 DPI (MSC-EVs). Using the rotarod, tightrope, and corner turn tests, we found that administration of both MSC lines and their MSC-EV fractions significantly enhanced motor coordination performance (Fig. 1). In all 4 experimental settings, the effects persisted over the entire observation period (i.e., 4 weeks after stroke induction; Fig. 1). We did not detect any significant differences in improved motor coordination impairment among the 4 treatment groups (i.e., the delivery of MSC-EVs was as effective as the transplantation of MSCs; Fig. 1).

MSC and MSC-EV Delivery Comparably Induce Postischemic Long-Term Neuroprotection

Because functional recovery does not necessarily imply an effect on brain tissue injury and vice versa, we subsequently analyzed neuronal survival in the ischemic striatum at 4 weeks after stroke. In line with the reduction of neurological impairment, increased densities of NeuN⁺ neurons (i.e., neuronal density) were found in the ischemic striatum of mice receiving MSCs or MSC-EV fractions. No statistically significant differences were observed between the mice treated with either MSCs or MSC-EVs (Fig. 2). On the contrary, MSC-EVs did not induce acute neuroprotection as assessed by determination of infarct volumes on days 2 and 6 post-stroke (supplemental online Fig. 3). The latter, however, might be due to the experimental paradigm chosen.

MSC and MSC-EV Delivery Similarly Increases Postischemic Angiogenesis

To elucidate whether MSC-EVs promote neurogenesis, we compared the effects of MSC and MSC-EV administration on cell proliferation 4 weeks after ischemia via BrdU incorporation. Compared with saline-treated stroke mice, more BrdU⁺ cells were identified within the ischemic striatum of those mice treated with either MSCs or MSC-EVs (Fig. 3). The numbers of immature (Dcx) and mature (NeuN) BrdU-labeled neuronal cell populations were both increased after MSC and MSC-EV treatment (Fig. 4A, 4B). Similarly, the numbers of CD31⁺ BrdU⁺ cells were elevated, indicating that new endothelial cells had also formed (Fig. 4C). Thus, MSC-EVs, like MSCs themselves, are able to induce postischemic angiogenesis. Again, no significant differences between the MSC-treated and MSC-EV-treated groups were recognized.

MSC-EVs Modulate Postischemic Peripheral Immune Responses

Evidence is emerging for an interaction between peripheral immune responses and postischemic inflammation in the brain that contributes to the development of ischemic brain injury [48]. Furthermore, the immune regulatory functions of MSCs and MSC-EVs are well established [42, 49]. Considering systemically administered MSC-EVs as the therapeutically active component of MSCs, we investigated whether stroke-induced peripheral immune responses are regulated by MSC-EVs. Therefore, we first determined the absolute cell counts of circulating leukocyte subsets in the blood. Because stroke-induced systemic immune responses are regulated in a time-dependent manner involving rapid acute activation [50] followed by suppression at subacute time points [51], we evaluated two time points (i.e., 2 and 6 DPI). The MSC-EV-treated stroke mice analyzed at 2 DPI had received a single MSC-EV injection at 24 hours after ischemia. The mice analyzed at 6 DPI had received 3 MSC-EV injections at 24 hours and 3 and 5 days.

Compared with sham-operated mice, absolute cell numbers of the total WBC count and neutrophil, dendritic cell, macrophage, monocyte (including different subsets), and lymphocyte subsets (including different T-lymphocyte subsets) were not altered at 2 DPI, neither in saline-treated nor in MSC-EV-treated mice (Fig. 5A–5H). However, we observed a twofold increase in the activation of CD4 and CD8 T lymphocytes in saline-treated stroke mice that was attenuated in the MSC-EV-treated mice, albeit the difference in the latter was not significant (Fig. 5J). A similar trend was observed in the activation of dendritic cells at this time point (Fig. 5F).

In contrast to these rather subtle changes at this early time point, we observed striking differences at 6 DPI. Saline-treated stroke mice (control) revealed only 50% of total WBCs in the peripheral blood compared with the level in the sham-operated mice (Fig. 6A). Mainly, the numbers of monocytes (75%) and the different lymphocyte subsets (60%–65%) were significantly decreased (Fig. 6E, 6G–6I). This phenomenon corresponds to stroke-induced immunosuppression and has been associated with poor neurological outcomes [52, 53]. The numbers of neutrophils, dendritic cells, and macrophages were not affected by focal cerebral ischemia (Fig. 6B–6D). In contrast to the saline-treated mice, the MSC-EV-treated mice showed almost normal numbers of B cells, NK cells, and T cells. However, the monocyte content was still reduced (Fig. 6E). Although the dendritic cell numbers were not significantly altered by focal cerebral ischemia, the content of MHC class II expressing dendritic cells (DCs) were significantly decreased in the saline-treated but not in the MSC-EV-treated mice (Fig. 6F). Similarly, a statistically significant increase in the numbers of CD4⁺ and CD8⁺ T cells expressing the activation marker CD69 was observed in saline-treated, but not in the MSC-EV-treated, mice (Fig. 6J). Thus, MSC-EV administration attenuates the effects of focal cerebral ischemia on the cellular composition of the peripheral blood system and the activation state of its cells.

Cerebral Immune Cell Infiltration Is not Modulated by MSC-EVs

Cerebral inflammatory processes contribute to secondary brain injury after stroke, involving numerous types of immune cells that infiltrate the brain at variable numbers exhibiting cell type-specific temporal and spatial distribution [54]. In order to characterize the effect of MSC-EVs on local brain inflammatory responses, we first performed an immunohistochemical analysis for CD45⁺ leukocytes to exclude potential confounding effects due to different sizes of evolving brain infarcts. With this approach, we did not detect any significant changes related to MSC-EV delivery, neither at 2 DPI nor at 6 DPI (Fig. 6A).

Because CD45 staining itself is not sufficient to discriminate cells of different hematopoietic subsets, we next performed multiparametric flow cytometric analysis of minced brain cells at 6 DPI (supplemental online Fig. 2). Peripheral blood leukocytes are known to express higher levels of CD45 than do microglial cells [54]. Quantification of total leukocyte numbers demonstrated a 4 times higher abundance in the ischemic tissue compared with the levels in the contralesional hemispheres ($n = 3$ experiments, each containing 4 pooled hemispheres; $p < .05$; Fig. 7B) and sham-operated mice. In line with immunohistochemical data, no effect of MSC-EV administration was observed

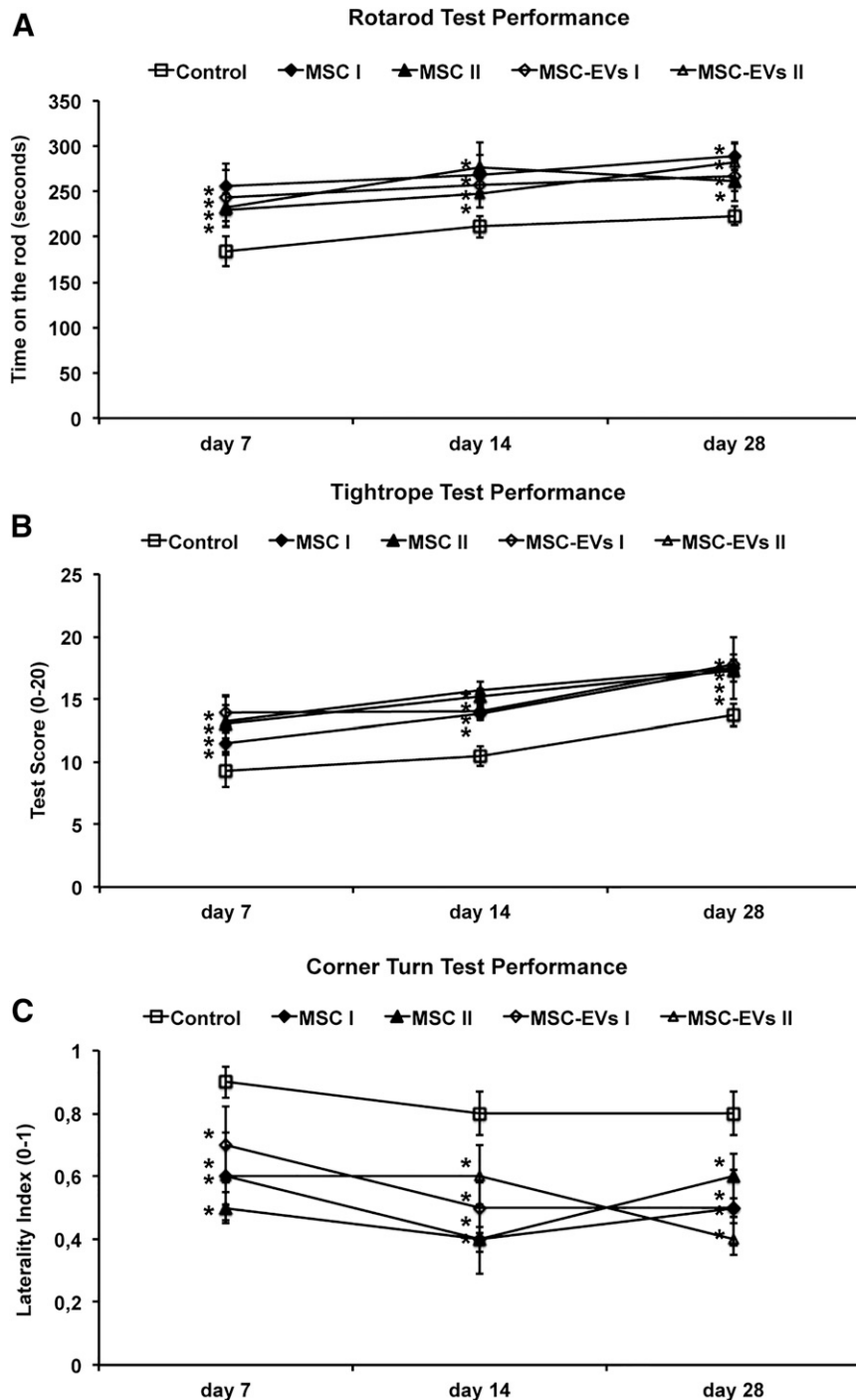


Figure 1. MSC-EVs reduce postischemic neurological impairment. Motor coordination, evaluated using the rotarod test (A), tightrope test (B), and corner turn test (C) at 7, 14, and 28 days after ischemia (DPI). Mice ($n = 12$ per condition) were exposed to middle cerebral artery occlusion, followed by delivery of normal saline (control), cells of 2 independent bone marrow-derived MSC lines (MSC I and MSC II), or EVs harvested from supernatants of both MSC lines (MSC-EVs I and MSC-EVs II). MSCs were infused at 1 DPI and MSC-EVs at 1, 3, and 5 DPI. MSC-EV-treated mice showed very similar neurological performance to that of MSC-treated mice. Data are mean \pm SD. *, $p < .05$ compared with control. Abbreviations: EVs, extracellular vesicles; MSC, mesenchymal stem cell; MSC I and MSC II, group I and II of bone marrow-derived MSC lines, respectively; MSC-EVs I and MSC-EVs II, supernatants of the two MSC lines.

on the recruitment of leukocytes into the infarcted brain hemispheres (Fig. 7B).

The absolute numbers of neutrophils, macrophages, monocytes, dendritic cells, and lymphocyte subtypes were determined for characterization of immune cell infiltration. The

most pronounced stroke-induced immune cell infiltration was observed for neutrophils and monocytes (Fig. 7C, 7F). The number of neutrophils in infarcted hemispheres was increased 12-fold compared with the number after sham surgery and in the contralesional hemispheres. The monocyte numbers had

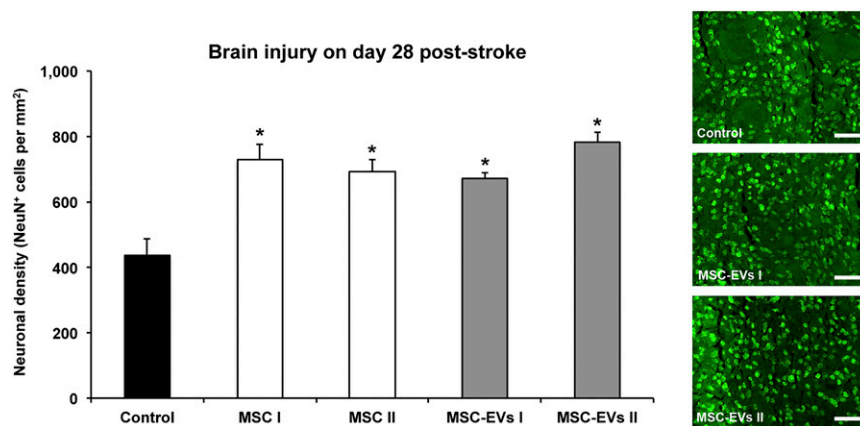


Figure 2. MSC-EVs induce postischemic long-term neuroprotection. Neuronal survival as examined by immunohistochemistry in the ischemic striatum at 28 days after ischemia in mice ($n = 12$ per condition) exposed to middle cerebral artery occlusion followed by i.v. delivery of normal saline (control), two different MSC lines (MSC I and MSC II), or their corresponding EVs (MSC-EVs I and MSC-EVs II). Representative microphotographs are also shown. Scale bars = $50 \mu\text{m}$. Data are mean \pm SD values. *, $p < .05$ compared with control. Abbreviations: EVs, extracellular vesicles; MSC, mesenchymal stem cell; MSC I and MSC II, group I and II of bone marrow-derived MSC lines, respectively; MSC-EVs I and MSC-EVs II, supernatants of the two MSC lines.

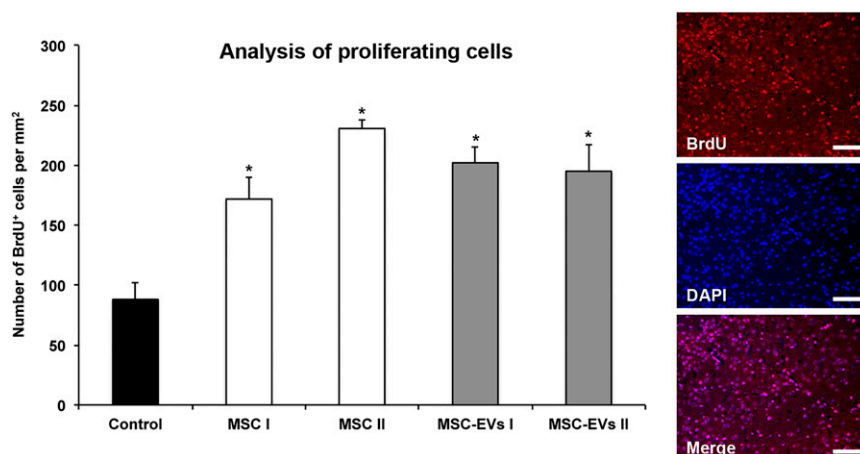


Figure 3. MSC-EVs increase postischemic cell proliferation. Cell proliferation was assessed by BrdU incorporation analysis in the ischemic striatum at 28 days after ischemia in mice ($n = 12$ per condition) exposed to middle cerebral artery occlusion followed by i.v. delivery of normal saline (control), cells of two independent bone marrow-derived MSC lines (MSC I and MSC II), or EVs harvested from supernatants of both MSC lines (MSC-EVs I and MSC-EVs II). Representative microphotographs of BrdU+ cells counterstained with DAPI are also shown. Scale bars = $100 \mu\text{m}$. Data are mean \pm SD values. *, $p < .05$ compared with control. Abbreviations: BrdU, 5-bromo-2-deoxyuridine; DAPI, 4',6'-diamidino-2-phenylindole; EVs, extracellular vesicles; MSC, mesenchymal stem cell; MSC I and MSC II, group I and II of bone marrow-derived MSC lines, respectively; MSC-EVs I and MSC-EVs II, supernatants of the two MSC lines.

increased by sixfold ($n = 3$ experiments, each containing 4 pooled hemispheres; $p < .05$). Less pronounced changes were observed for dendritic cells and macrophages. Similarly, T and B lymphocytes increased by 1.5-fold to 3-fold ($n = 3$ experiments, each containing 4 pooled hemispheres; $p < .05$; Fig. 7H). MSC-EV administration did not modulate infiltration of any of these cell types (Fig. 7C–7F, 7H). Moreover, the proportions of monocyte and T-cell subsets and activation of monocytes, dendritic cells, B cells, and CD8+ T cells were not influenced by the administration of MSC-EVs (Fig. 7F, 7G, 7I).

DISCUSSION

We have shown that MSC-EVs improve postischemic neurological impairment very similarly to MSCs and induce long-term neuroprotection

associated with enhanced angiogenesis. The latter persisted throughout the observation period of 4 weeks. In line with previous reports on transplanted MSCs, our data have shown that MSCs exert their restorative properties in a paracrine manner rather than by direct cellular interaction [23, 24, 30]. Consequently, our data have identified EVs as a key component via which MSCs promote post-stroke recovery. In good agreement with previous reports showing MSCs and MSC-EVs as modulators of immune functions [42, 49], we found that postischemic immunosuppression (i.e., B-cell, NK-cell, and T-cell lymphopenia) is attenuated in the peripheral blood by MSC-EVs. Our data thus suggest that MSC-EVs' immunomodulatory effects might contribute to establish an appropriate external milieu for successful brain remodeling.

MSCs have been repeatedly shown to induce neuroprotection, most likely via indirect mechanisms in various stroke models. As

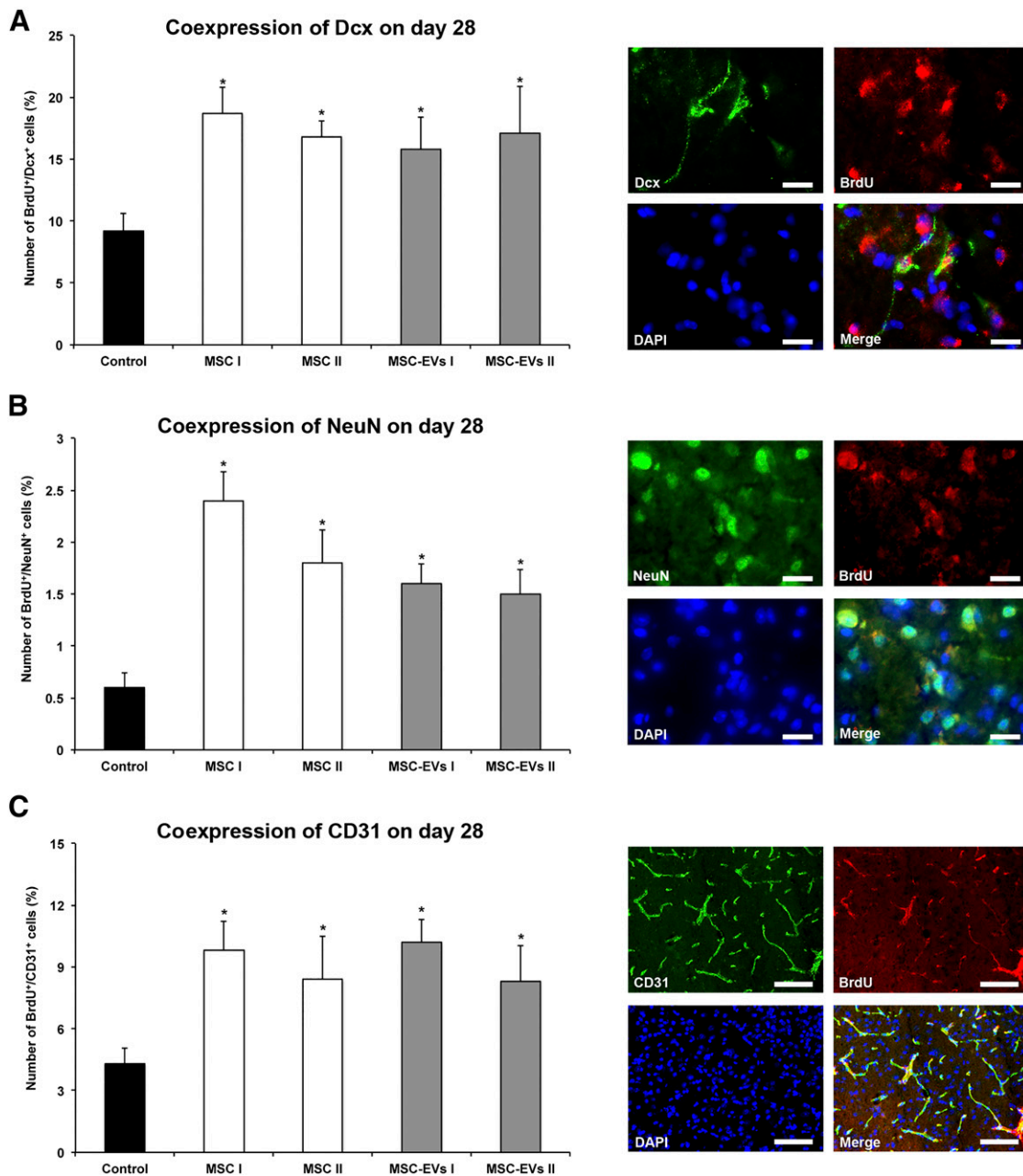


Figure 4. MSC-EVs stimulate postischemic neurogenesis and angiogenesis. Double-immunohistochemistry for the proliferation marker BrdU and the immature neuronal marker Dcx (**A**), the proliferation marker BrdU and the mature neuronal marker NeuN (**B**), and the proliferation marker BrdU and the endothelial marker CD31 (**C**), evaluated in the ischemic striatum at 28 days after ischemia. Mice ($n = 12$ per condition) were exposed to middle cerebral artery occlusion followed by i.v. delivery of normal saline (control), cells of two independent bone marrow-derived MSCs lines (MSC I and MSC II), or EVs harvested from supernatants of both MSC lines (MSC-EVs I and MSC-EVs II). Representative microphotographs of double-labeled cells counterstained with DAPI are also shown. Scale bars = 20 μm . Data are mean \pm SD values. *, $p < .05$ compared with control. Abbreviations: BrdU, 5-bromo-2-deoxyuridine; DAPI, 4',6-diamidino-2-phenylindole; Dcx, doublecortin; EVs, extracellular vesicles; MSC, mesenchymal stem cell; MSC I and MSC II, group I and II of bone marrow-derived MSC lines, respectively; MSC-EVs I and MSC-EVs II, supernatants of the two MSC lines.

such, the beneficial effects of MSC-EV administration on motor coordination deficits after focal cerebral ischemia in rats have recently been demonstrated [32]. The present study goes beyond the latter study, demonstrating equivalence of EVs and BM-derived MSCs. Whether MSCs and/or EVs from other tissue sources such as adipose tissue, which facilitates MSC generation compared with BM, might have similar effects was beyond the scope of the present work. We found delayed neuroprotection and a possible

mechanism of EV action (i.e., the reversal of postischemic immunosuppression, most specifically of B-cell, NK-cell, and T-cell lymphopenia). Both MSC-EVs and MSCs increased neuronal survival in the peri-infarct tissue, as revealed at the end of the observation period at 28 DPI. Because long-term neuronal survival might be a consequence of both early and delayed neuroprotection, we also analyzed ischemic injury at 2 and 6 DPI but failed to detect an effect of EVs on infarct volume at these early time points. Although MSC

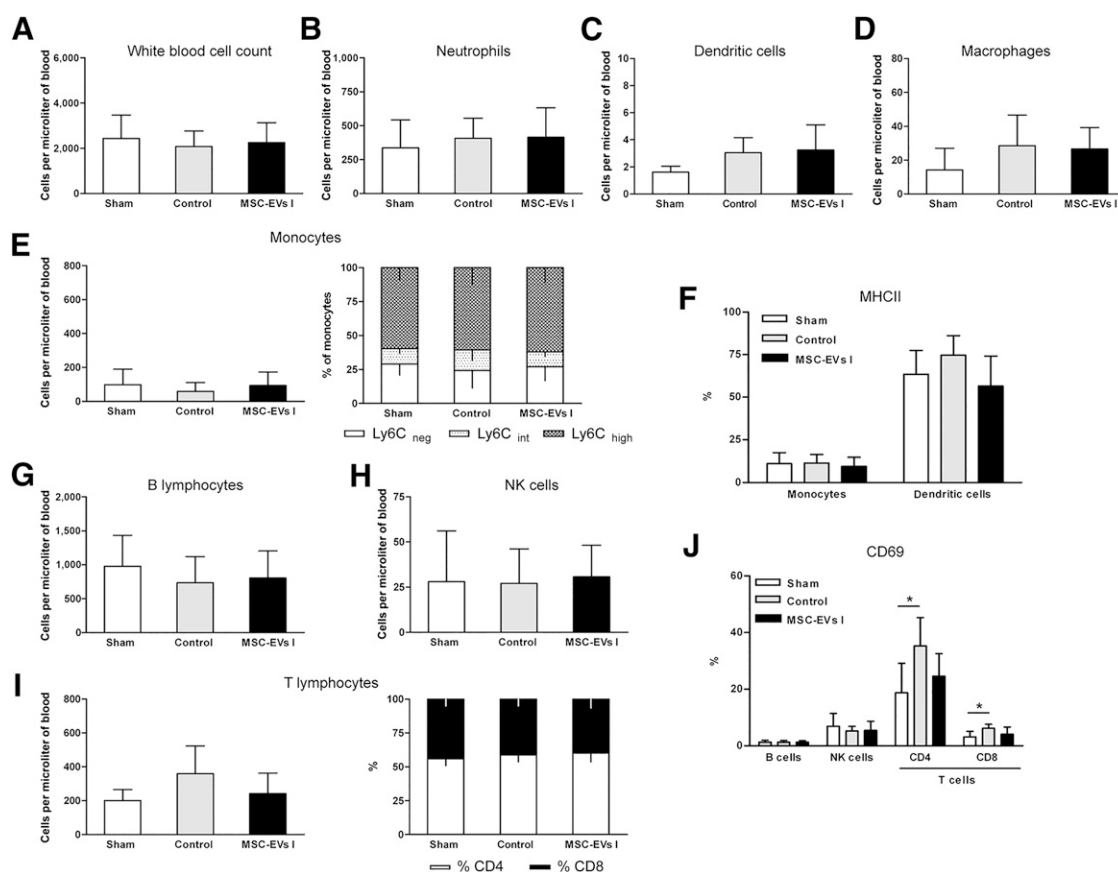


Figure 5. MSC-EVs do not influence acute immune responses at 2 days after ischemia. Absolute counts and relative proportions of peripheral blood leukocytes and leukocyte subsets at 48 hours after ischemia or sham surgery ($n = 8$ per condition). Sham-operated mice underwent the same operation procedure as for ischemia, except for occlusion of the middle cerebral artery. Normal saline (control) or EVs harvested from supernatants of MSC line I (MSC-EVs I) were i.v. delivered to mice exposed to middle cerebral artery occlusion at 24 hours after ischemia; sham mice received saline injections. **(A):** Total white blood cell counts were analyzed using a veterinary hematology analyzer. The absolute cell numbers of neutrophils **(B)**, dendritic cells **(C)**, macrophages **(D)**, monocytes **(E)**, and monocyte subsets [B lymphocytes **(G)**, NK cells **(H)**, and T lymphocytes **(I)**] were determined by flow cytometry. The proportion of inflammatory ($Ly6C^{high}$) and resident ($Ly6C^{neg}$) monocytes **(E, right)** and that of CD4 and CD8 T lymphocytes **(I, right)** was also calculated. Activation of myeloid cells (monocytes and dendritic cells) **(F)** and lymphocytes **(J)** was evaluated by MHCII and CD69 expression analysis, respectively. Specifications of leukocyte subset identification according to their specific antigen expression are listed in the supplemental online Table 1 and show in supplemental online Figure 2. Data are mean \pm SD values. *, $p < .05$ compared with sham surgery. Abbreviations: EVs, extracellular vesicles; MHCII, major histocompatibility class II; MSC, mesenchymal stem cell; MSC I and MSC II, group I and II of bone marrow-derived MSC lines, respectively; MSC-EVs I and MSC-EVs II, supernatants of the two MSC lines; NK, natural killer.

transplantation has previously been shown to reduce infarct volume [55–57], this effect on infarct size strongly depends on cell transplantation timing [58]. Hence, the delivery of MSC-EVs at 1 DPI was obviously too late to prevent the progression of brain infarction. That MSC-EV delivery nonetheless promoted neurological recovery and prevented secondary neurodegeneration emphasizes its therapeutic potential in the subacute and postacute stroke phase (e.g., as add-on treatment to thrombolysis). That i.v. EV delivery was sufficient to induce post-stroke neuroprotection and neurological recovery again highlights the putative clinical impact of EVs in future stroke treatment, albeit other delivery routes were not studied in the present work. In this context, systemic post-stroke delivery such as i.v. injection is most feasible in clinical terms and not inferior to local stereotactic delivery, which has been previously observed by our group in a model of post-stroke neural progenitor cell transplantation in mice (unpublished data).

Although stem and progenitor cells are integrated to a very limited extent into residing neural networks [1, 7, 58, 59], grafted cells such as MSCs and neural progenitor cells are known to

stimulate brain remodeling and to promote angiogenesis via indirect bystander effects [1, 5, 22, 60]. MSC-EVs share this MSC property, inducing angiogenesis as we have shown and as was also demonstrated previously [32]. The precise mechanisms underlying stimulation of angiogenesis due to grafted stem cells or EVs are still elusive. Yet, transplanted cells, such as neural progenitor cells, have been described to modify the post-stroke microenvironment in terms of growth factor contents and enhanced post-stroke neurogenesis [22]. In this sense, EVs might have similar effects that might depend on their content's composition. Defining the precise composition of EVs was, however, beyond the scope of the present study. It is unlikely that a single EV mediator such as growth factors or microRNAs, which also induce post-stroke neurogenesis per se [61], is responsible for these effects. Rather, we hypothesized that a complex interplay between hitherto not fully elucidated EV contents and host responses are crucially involved in this process. Nevertheless, the shared mechanisms of action reveal the high similarity of MSC-EVs and MSCs, suggesting that MSC-EVs

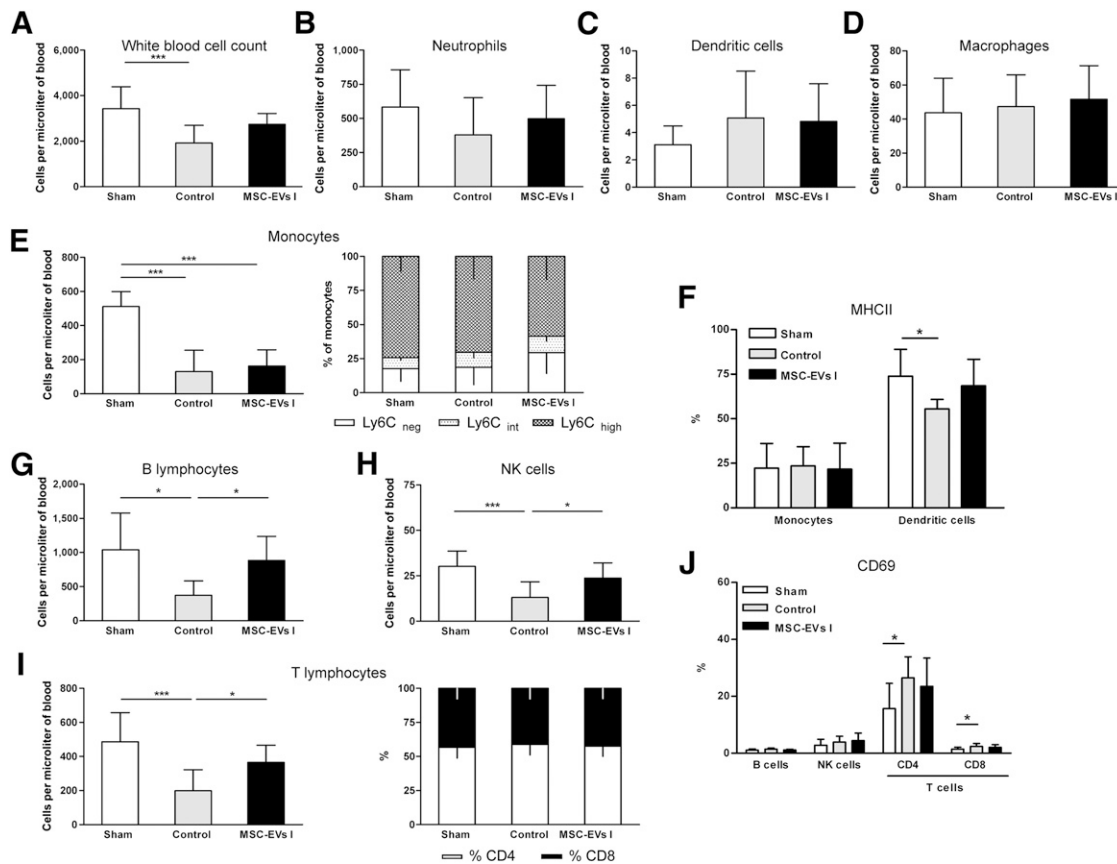


Figure 6. MSC-EVs reverse postischemic lymphopenia at 6 days after ischemia. Absolute counts and relative proportions of peripheral blood leukocytes and leukocyte subsets at 6 days after ischemia or after sham surgery ($n = 12$ per condition). Sham-operated mice underwent the same operation procedure as for ischemia except for occlusion of the middle cerebral artery. Normal saline (control) or EVs harvested from supernatants of MSC line I (MSC-EVs I) were i.v. delivered to mice exposed to middle cerebral artery occlusion (MCAO) at 1, 3, and 5 days after ischemia; sham mice received saline injections. **(A):** Total white blood cell counts were analyzed using a veterinary hematology analyzer. Absolute cell numbers of neutrophils **(B)**, dendritic cells **(C)**, macrophages **(D)**, monocytes **(E)**, B lymphocytes **(G)**, NK cells **(H)**, and T lymphocytes **(I)** were determined by flow cytometry. The proportion of inflammatory ($\text{Ly6C}^{\text{high}}$) and resident (Ly6C^{neg}) monocytes **(E, right)** and of CD4 and CD8 T lymphocytes **(I, right)** was also calculated. Activation of myeloid cells (monocytes and dendritic cells) **(F)** and lymphocytes **(J)** was evaluated by MHCII and CD69 expression analysis, respectively. Specifications of leukocyte subset identification according to their specific antigen expression are listed in supplemental online Table 1 and show in in supplemental online Figure 2. Data are mean \pm SD. *, $p < .05$ or ***, $p < .001$ compared with sham surgery or MCAO. Abbreviations: EVs, extracellular vesicles; MHCII, major histocompatibility class II; MSC, mesenchymal stem cell; MSC I and MSC II, group I and II of bone marrow-derived MSC lines, respectively; MSC-EVs I and MSC-EVs II, supernatants of the two MSC lines; NK, natural killer.

might represent the therapeutically active component of MSCs. Recent data have suggested that stimulation of angiogenesis is critical for MSC-induced postischemic neuroprotection [62]. It is therefore not surprising that neurological improvement, neuroprotection, and angiogenesis went in line with each other.

MSCs are called immunologically inert but able to modulate both peripheral and cerebral immune responses. Immunological responses rather than direct intercalation of MSCs with brain structures have been made responsible for restorative effects of MSCs [63, 64]. Thus, injection of conditioned media obtained from MSC cultures suppressed inflammation as efficiently as MSCs in models of kidney and myocardial injury [24, 65]. Based on these observations, we hypothesized that MSC-EV delivery modulated the postischemic peripheral and cerebral immune responses. Stroke is followed by a phase of immunosuppression [66] that predisposes the body to infection and neurological deterioration [51, 53]. With this knowledge, we suspected that the anti-inflammatory actions of MSC-EVs might have aggravated postischemic

immunodeficiency, which might have led to detrimental stroke outcomes. In contrast to this assumption, our results showed that MSC-EVs did not exacerbate, but attenuated, postischemic lymphopenia at 6 DPI, which is a hallmark of post-stroke immunosuppression [51, 52]. Thus, the total numbers of B cells, NK cells, and T cells were consistently elevated by EV delivery (i.e., to levels very similar to those of the sham-operated mice).

Concomitant with the normalization of B cells, NK cells, and T cells, a deactivation of DCs and residual T cells, which were activated in normal saline-treated stroke mice, was observed in the MSC-EV-treated stroke mice. Although an increased activation of immune effector cells might initially appear to be contradictory to the phenomenon of postischemic immunosuppression, a similar coincidence has been observed in human stroke patients [67]. As such, these data are consistent with our previous observation that MSC-EVs reversed T-cell responses derived from a steroid refractory GvHD patient toward allogeneic target cells, independent of whether they were treated with MSC-EVs in vitro or were taken from the patient during MSC-EV therapy [42].

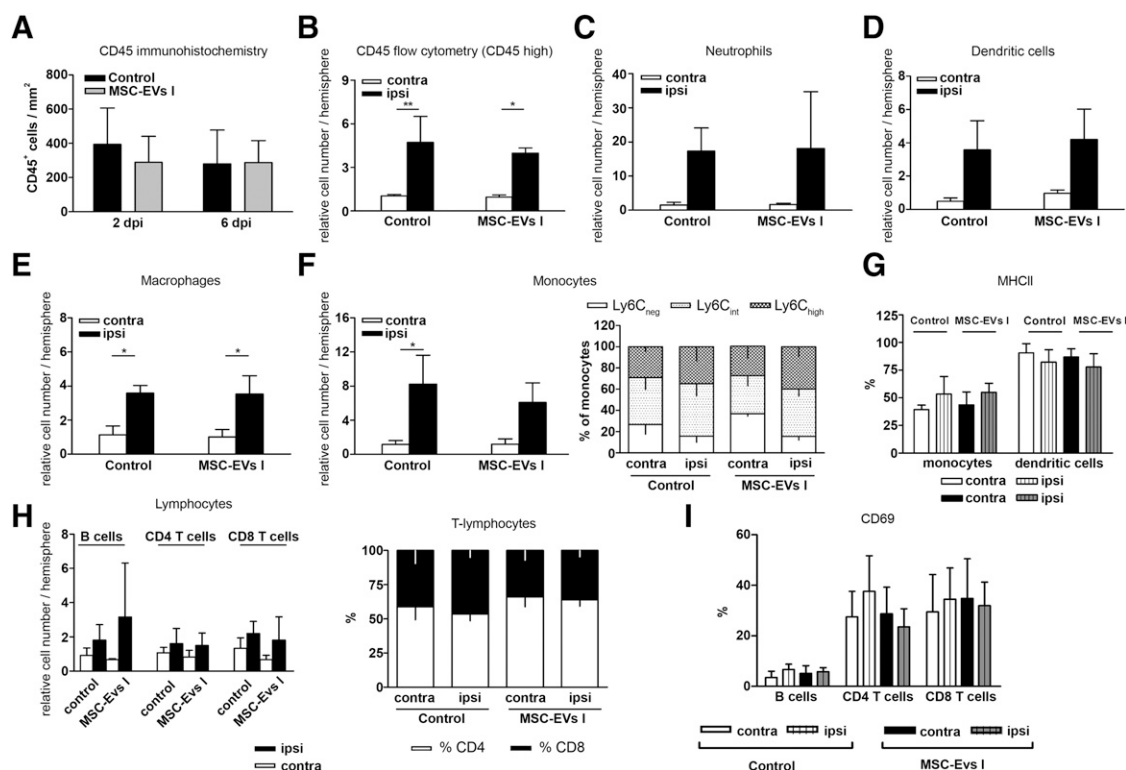


Figure 7. Cerebral immune cell infiltration is not modulated by MSC-EVs. **(A):** Density of leukocytes in the ischemic striatum at 2 and 6 days after ischemia (DPI) evaluated by CD45 immunohistochemistry ($n = 8$ per condition). Total number of CD45⁺ leukocytes **(B)**, neutrophils **(C)**, dendritic cells **(D)**, macrophages **(E)**, monocytes **(F)**, and lymphocytes **(H)** in the ipsilateral and contralateral hemisphere at 6 DPI as determined by flow cytometry. Activation of myeloid subsets **(G)** and lymphocyte subsets **(I)** as determined by MHCII and CD69 expression analysis in the ipsilateral and contralateral hemisphere at 6 DPI using flow cytometry in mice exposed to middle cerebral artery occlusion, followed by i.v. delivery of normal saline (control) or EVs harvested from supernatants of MSC line I (MSC-EVs I) at 1, 3, and 5 DPI. In the proportion of monocyte **(F)** and T lymphocyte **(H)** subsets was also measured. Three independent flow cytometry experiments were performed, for each of which four brain hemispheres per group were pooled. Data are mean \pm SD. *, $p < .05$ or **, $p < .01$ compared with the contralateral hemisphere. Abbreviations: contra, contralateral; EVs, extracellular vesicles; ipsi, ipsilateral; MHCII, major histocompatibility class II; MSC, mesenchymal stem cell; MSC I and MSC II, group I and II of bone marrow-derived MSC lines, respectively; MSC-EVs I and MSC-EVs II, supernatants of the two MSC lines; NK, natural killer.

Although recent studies have documented that MSC transplantation dampens cerebral inflammation [59, 68], we did not observe differences in stroke-induced brain immune cell infiltrates after EV delivery. This is in contrast to previous studies, in which MSCs were transplanted in stroke mice, resulting in reduced brain leukocyte infiltration [69]. However, in the absence of proinflammatory cytokines and sufficient nitric oxide production, MSCs instead have immune-stimulatory effects (e.g., through stimulation of T-cell proliferation) [70]. Because the EV fractions used in the present study were derived from nonstimulated MSC cultures, it is conceivable that their anti-inflammatory action was too low to prevent brain leukocyte infiltration.

CONCLUSION

Because of the desirable translation of MSC-EVs from bench to bedside and considering the clinical trials with MSC-EVs in human stroke patients, additional studies are urgently required to define whether MSC-EVs (and in EVs in general) are able to enter the brain. If (as we have postulated) EVs indeed mediate their restorative action by equilibrating peripheral immune responses, blood measurements might provide an elegant strategy for monitoring the therapeutic responses to MSC-EVs. We predict that with

stringent proof-of-concept strategies, it might be possible to translate MSC-EV therapy from rodents to human patients, because MSC-EVs are more suitable for clinical application than is transplantation of (undifferentiated) stem cells. After a myriad of study failures, the stroke field might greatly benefit from a clinically applicable therapeutic strategy, for which the scientific community has eagerly waited.

ACKNOWLEDGMENTS

This work was supported by the Volkswagen Foundation (to T.R.D., D.M.H., and B.G.), the Forschungsförderung Essen program of the Medical Faculty of the University of Duisburg-Essen (to T.R.D.), and the German Research Council (Grants HE3173/2-2 and HE3173/3-1 to D.M.H.). We thank Britta Kaltwasser for excellent technical assistance and Dr. Lambros Kordelas and the Stem Cell Department of the Red Cross Blood Service West for kindly providing bone marrow samples to raise mesenchymal stem cells.

AUTHOR CONTRIBUTIONS

T.R.D.: conception/design, financial support, collection and/or assembly of data, data analysis and interpretation, manuscript

writing, final approval of manuscript; J.H.: conception/design, collection and/or assembly of data, data analysis and interpretation, manuscript writing, final approval of manuscript; A.G.: collection and/or assembly of data, data analysis and interpretation, final approval of manuscript; J.S., A.-K.L., S.R., and K.d.M.: collection and/or assembly of data, final approval of manuscript; P.A.H.: administrative support, manuscript writing, final approval of manuscript; B.G.: conception/design, financial support, data analysis and interpretation, manuscript writing, final approval of manuscript; D.M.H.: conception/design, financial

support, administrative support, manuscript writing, final approval of manuscript.

DISCLOSURE OF POTENTIAL CONFLICTS OF INTEREST

P.A.H. has a patent pending for "Use of preparations comprising exosomes derived from mesenchymal stem cells (MSCs) in the prevention and therapy of inflammatory conditions" (EP000002687219A1). The other authors indicated no potential conflicts of interest.

REFERENCES

- Bacigaluppi M, Pluchino S, Peruzzotti-Jametti L et al. Delayed post-ischaemic neuroprotection following systemic neural stem cell transplantation involves multiple mechanisms. *Brain* 2009;132:2239–2251.
- Banerjee S, Williamson DA, Habib N et al. The potential benefit of stem cell therapy after stroke: An update. *Vasc Health Risk Manag* 2012;8:569–580.
- Chen J, Li Y, Wang L et al. Therapeutic benefit of intravenous administration of bone marrow stromal cells after cerebral ischemia in rats. *Stroke* 2001;32:1005–1011.
- Dharmasaroja P. Bone marrow-derived mesenchymal stem cells for the treatment of ischemic stroke. *J Clin Neurosci* 2009;16:12–20.
- Doepfner TR, Kaltwasser B, Teli MK et al. Effects of acute versus post-acute systemic delivery of neural progenitor cells on neurological recovery and brain remodeling after focal cerebral ischemia in mice. *Cell Death Dis* 2014;5:e1386.
- Leong WK, Henshall TL, Arthur A et al. Human adult dental pulp stem cells enhance post-stroke functional recovery through non-neural replacement mechanisms. *STEM CELLS TRANSLATIONAL MEDICINE* 2012;1:177–187.
- Schwartz S, Litwak S, Hao W et al. Hematopoietic stem cells reduce postischemic inflammation and ameliorate ischemic brain injury. *Stroke* 2008;39:2867–2875.
- Shen LH, Li Y, Chen J et al. One-year follow-up after bone marrow stromal cell treatment in middle-aged female rats with stroke. *Stroke* 2007;38:2150–2156.
- Shen LH, Li Y, Chen J et al. Therapeutic benefit of bone marrow stromal cells administered 1 month after stroke. *J Cereb Blood Flow Metab* 2007;27:6–13.
- Shen LH, Li Y, Chen J et al. Intracarotid transplantation of bone marrow stromal cells increases axon-myelin remodeling after stroke. *Neuroscience* 2006;137:393–399.
- Ukai R, Honmou O, Harada K et al. Mesenchymal stem cells derived from peripheral blood protect against ischemia. *J Neurotrauma* 2007;24:508–520.
- Zheng W, Honmou O, Miyata K et al. Therapeutic benefits of human mesenchymal stem cells derived from bone marrow after global cerebral ischemia. *Brain Res* 2010;1310:8–16.
- Caplan AI. Adult mesenchymal stem cells for tissue engineering versus regenerative medicine. *J Cell Physiol* 2007;213:341–347.
- Bhasin A, Srivastava MV, Kumaran SS et al. Autologous mesenchymal stem cells in chronic stroke. *Cerebrovasc Dis Extra* 2011;1:93–104.
- Bhasin A, Srivastava MV, Mohanty S et al. Stem cell therapy: A clinical trial of stroke. *Clin Neurol Neurosurg* 2013;115:1003–1008.
- Doepfner TR, Hermann DM. Stem cell-based treatments against stroke: Observations from human proof-of-concept studies and considerations regarding clinical applicability. *Front Cell Neurosci* 2014;8:357.
- Honmou O, Houkin K, Matsunaga T et al. Intravenous administration of auto serum-expanded autologous mesenchymal stem cells in stroke. *Brain* 2011;134:1790–1807.
- Savitz SI, Misra V, Kasam M et al. Intravenous autologous bone marrow mononuclear cells for ischemic stroke. *Ann Neurol* 2011;70:59–69.
- England T, Martin P, Bath PM. Stem cells for enhancing recovery after stroke: A review. *Int J Stroke* 2009;4:101–110.
- Hermann DM, Chopp M. Promoting brain remodelling and plasticity for stroke recovery: Therapeutic promise and potential pitfalls of clinical translation. *Lancet Neurol* 2012;11:369–380.
- Yoo SW, Kim SS, Lee SY et al. Mesenchymal stem cells promote proliferation of endogenous neural stem cells and survival of newborn cells in a rat stroke model. *Exp Mol Med* 2008;40:387–397.
- Doepfner TR, Ewert TA, Tönges L et al. Transduction of neural precursor cells with TAT-heat shock protein 70 chaperone: Therapeutic potential against ischemic stroke after intrastriatal and systemic transplantation. *STEM CELLS* 2012;30:1297–1310.
- Lee RH, Pulin AA, Seo MJ et al. Intravenous hMSCs improve myocardial infarction in mice because cells embolized in lung are activated to secrete the anti-inflammatory protein TSG-6. *Cell Stem Cell* 2009;5:54–63.
- Timmers L, Lim SK, Arslan F et al. Reduction of myocardial infarct size by human mesenchymal stem cell conditioned medium. *Stem Cell Res (Amst)* 2007;1:129–137.
- Hsieh JY, Wang HW, Chang SJ et al. Mesenchymal stem cells from human umbilical cord express preferentially secreted factors related to neuroprotection, neurogenesis, and angiogenesis. *PLoS One* 2013;8:e72604.
- Scheibe F, Klein O, Klose J et al. Mesenchymal stromal cells rescue cortical neurons from apoptotic cell death in an in vitro model of cerebral ischemia. *Cell Mol Neurobiol* 2012;32:567–576.
- Tate CC, Fonck C, McGrogan M et al. Human mesenchymal stromal cells and their derivative, SB623 cells, rescue neural cells via trophic support following in vitro ischemia. *Cell Transplant* 2010;19:973–984.
- Cantaluppi V, Gatti S, Medica D et al. Microvesicles derived from endothelial progenitor cells protect the kidney from ischemia-reperfusion injury by microRNA-dependent reprogramming of resident renal cells. *Kidney Int* 2012;82:412–427.
- Gatti S, Bruno S, Derigibus MC et al. Microvesicles derived from human adult mesenchymal stem cells protect against ischaemia-reperfusion-induced acute and chronic kidney injury. *Nephrol Dial Transplant* 2011;26:1474–1483.
- Lai RC, Arslan F, Lee MM et al. Exosome secreted by MSC reduces myocardial ischemia/reperfusion injury. *Stem Cell Res (Amst)* 2010;4:214–222.
- Li T, Yan Y, Wang B et al. Exosomes derived from human umbilical cord mesenchymal stem cells alleviate liver fibrosis. *Stem Cells Dev* 2013;22:845–854.
- Xin H, Li Y, Cui Y et al. Systemic administration of exosomes released from mesenchymal stromal cells promote functional recovery and neurovascular plasticity after stroke in rats. *J Cereb Blood Flow Metab* 2013;33:1711–1715.
- Witwer KW, Buzás EI, Bemis LT et al. Standardization of sample collection, isolation and analysis methods in extracellular vesicle research. *J Extracell Vesicles* 2013;2:2.
- Thery C, Amigorena S, Raposo G et al. Isolation and characterization of exosomes from cell culture supernatants and biological fluids. *Curr Protoc Cell Biol* 2006;Chapter 3:Unit 3.22.
- Valadi H, Ekström K, Bossios A et al. Exosome-mediated transfer of mRNAs and microRNAs is a novel mechanism of genetic exchange between cells. *Nat Cell Biol* 2007;9:654–659.
- Ludwig AK, Giebel B. Exosomes: Small vesicles participating in intercellular communication. *Int J Biochem Cell Biol* 2012;44:11–15.
- Mitkari B, Kerkelä E, Nystedt J et al. Intra-arterial infusion of human bone marrow-derived mesenchymal stem cells results in transient localization in the brain after cerebral ischemia in rats. *Exp Neurol* 2013;239:158–162.
- Janowski M, Lyczek A, Engels C et al. Cell size and velocity of injection are major determinants of the safety of intracarotid stem cell transplantation. *J Cereb Blood Flow Metab* 2013;33:921–927.
- Blum B, Benvenisty N. The tumorigenicity of human embryonic stem cells. *Adv Cancer Res* 2008;100:133–158.
- Blum B, Benvenisty N. The tumorigenicity of diploid and aneuploid human pluripotent stem cells. *Cell Cycle* 2009;8:3822–3830.
- Dlouhy BJ, Awe O, Rao RC et al. Autograft-derived spinal cord mass following olfactory mucosal cell transplantation in a spinal cord injury patient: Case report. *J Neurosurg Spine* 2014;21:618–622.
- Kordelas L, Rebmann V, Ludwig AK et al. MSC-derived exosomes: A novel tool to treat therapy-refractory graft-versus-host disease. *Leukemia* 2014;28:970–973.
- Le Blanc K, Rasmusson I, Sundberg B et al. Treatment of severe acute graft-versus-host

disease with third party haploidentical mesenchymal stem cells. *Lancet* 2004;363:1439–1441.

44 Sokolova V, Ludwig AK, Hornung S et al. Characterisation of exosomes derived from human cells by nanoparticle tracking analysis and scanning electron microscopy. *Colloids Surf B Biointerfaces* 2011;87:146–150.

45 Doepfner TR, Kaltwasser B, Bähr M et al. Effects of neural progenitor cells on post-stroke neurological impairment—A detailed and comprehensive analysis of behavioral tests. *Front Cell Neurosci* 2014;8:338.

46 Lin TN, He YY, Wu G et al. Effect of brain edema on infarct volume in a focal cerebral ischemia model in rats. *Stroke* 1993;24:117–121.

47 Herz J, Hagen SI, Bergmüller E et al. Exacerbation of ischemic brain injury in hypercholesterolemic mice is associated with pronounced changes in peripheral and cerebral immune responses. *Neurobiol Dis* 2014;62:456–468.

48 Macrez R, Ali C, Toutirais O et al. Stroke and the immune system: From pathophysiology to new therapeutic strategies. *Lancet Neurol* 2011;10:471–480.

49 Uccelli A, Moretta L, Pistoia V. Mesenchymal stem cells in health and disease. *Nat Rev Immunol* 2008;8:726–736.

50 Offner H, Subramanian S, Parker SM et al. Experimental stroke induces massive, rapid activation of the peripheral immune system. *J Cereb Blood Flow Metab* 2006;26:654–665.

51 Dirnagl U, Klehmet J, Braun JS et al. Stroke-induced immunodepression: Experimental evidence and clinical relevance. *Stroke* 2007;38(Suppl):770–773.

52 Meisel C, Meisel A. Suppressing immunosuppression after stroke. *N Engl J Med* 2011;365:2134–2136.

53 Meisel C, Schwab JM, Prass K et al. Central nervous system injury-induced immune deficiency syndrome. *Nat Rev Neurosci* 2005;6:775–786.

54 Gelderblom M, Leypoldt F, Steinbach K et al. Temporal and spatial dynamics of cerebral immune cell accumulation in stroke. *Stroke* 2009;40:1849–1857.

55 Chung DJ, Choi CB, Lee SH et al. Intraterrially delivered human umbilical cord blood-derived mesenchymal stem cells in canine cerebral ischemia. *J Neurosci Res* 2009;87:3554–3567.

56 Honma T, Honmou O, Iihoshi S et al. Intravenous infusion of immortalized human mesenchymal stem cells protects against injury in a cerebral ischemia model in adult rat. *Exp Neurol* 2006;199:56–66.

57 Leu S, Lin YC, Yuen CM et al. Adipose-derived mesenchymal stem cells markedly attenuate brain infarct size and improve neurological function in rats. *J Transl Med* 2010;8:63.

58 Bliss TM, Andres RH, Steinberg GK. Optimizing the success of cell transplantation therapy for stroke. *Neurobiol Dis* 2010;37:275–283.

59 Doepfner TR, Hermann DM. Mesenchymal stem cells in the treatment of ischemic stroke: Progress and possibilities. *Stem Cells Cloning* 2010;3:157–163.

60 Onda T, Honmou O, Harada K et al. Therapeutic benefits by human mesenchymal stem cells (hMSCs) and Ang-1 gene-modified hMSCs after cerebral ischemia. *J Cereb Blood Flow Metab* 2008;28:329–340.

61 Doepfner TR, Doehring M, Bretschneider E et al. MicroRNA-124 protects against focal cerebral ischemia via mechanisms involving

Usp14-dependent REST degradation. *Acta Neuropathol* 2013;126:251–265.

62 Komatsu K, Honmou O, Suzuki J et al. Therapeutic time window of mesenchymal stem cells derived from bone marrow after cerebral ischemia. *Brain Res* 2010;1334:84–92.

63 Caplan AI, Correa D. The MSC: An injury drugstore. *Cell Stem Cell* 2011;9:11–15.

64 Pittenger M. Sleuthing the source of regeneration by MSCs. *Cell Stem Cell* 2009;5:8–10.

65 van Koppen A, Joles JA, van Balkom BW et al. Human embryonic mesenchymal stem cell-derived conditioned medium rescues kidney function in rats with established chronic kidney disease. *PLoS One* 2012;7:e38746.

66 Famakin BM. The immune response to acute focal cerebral ischemia and associated post-stroke immunodepression: A focused review. *Aging Dis* 2014;5:307–326.

67 Vogelgesang A, May VE, Grunwald U et al. Functional status of peripheral blood T-cells in ischemic stroke patients. *PLoS One* 2010;5:e8718.

68 Sheikh AM, Nagai A, Wakabayashi K et al. Mesenchymal stem cell transplantation modulates neuroinflammation in focal cerebral ischemia: Contribution of fractalkine and IL-5. *Neurobiol Dis* 2011;41:717–724.

69 Yoo SW, Chang DY, Lee HS et al. Immune following suppression mesenchymal stem cell transplantation in the ischemic brain is mediated by TGF- β . *Neurobiol Dis* 2013;58:249–257.

70 Li W, Ren G, Huang Y et al. Mesenchymal stem cells: A double-edged sword in regulating immune responses. *Cell Death Differ* 2012;19:1505–1513.



See www.StemCellsTM.com for supporting information available online.